Supporting information

Hydration and Ion Pairing in Aqueous Mg^{2+} and Zn^{2+} Solutions: Force Field Description Aided by Neutron Scattering Experiments and *Ab Initio* Molecular Dynamics Simulations

Elise Duboué-Dijon,*,† Philip E. Mason,*,† Henry E. Fischer,‡ and Pavel Jungwirth*,†

†*Institute of Organic Chemistry and Biochemistry, Czech Academy of Sciences, Flemingovo nam. 2, 16610 Prague 6, Czech Republic*

‡*Institut Laue-Langevin, 71 Avenue des Martyrs, CS 20156, 38042 Grenoble Cedex 9, France*

E-mail: elise.duboue-dijon@uochb.cas.cz; philip.mason@uochb.cas.cz; pavel.jungwirth@uochb.cas.cz

Neutron scattering experiments

Fig. S1a shows the first order differences $\Delta S^{Mg-W}(Q)$, $\Delta S^{Zn-W}(Q)$, and $\Delta S^{Mg-Zn}(Q)$ before and after removal of the residual Placzek background using Fourier filtering. The substracted background (Fig. S1b) does not exhibit any structured features, which validates the employed procedure. Two spurious peaks due to noisy detectors were deleted in $\Delta S^{Mg-W}(Q)$ and

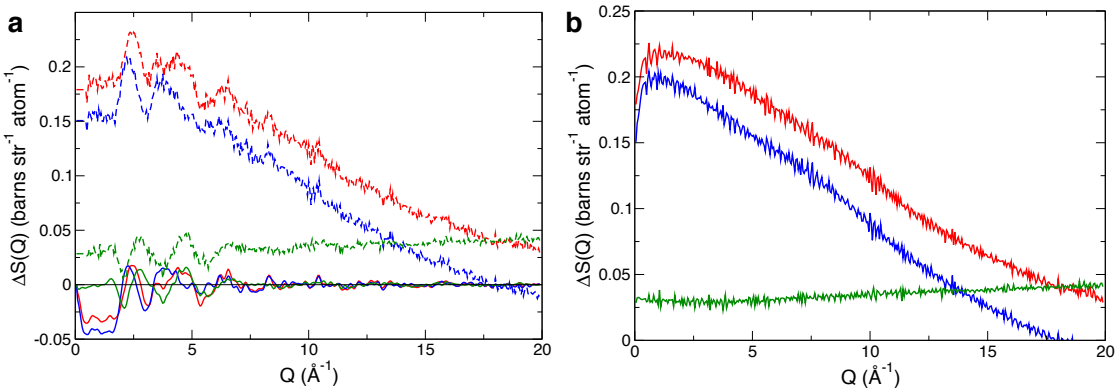

Figure S1: a) First order difference structure factore before (dashes) and after (solid lines) Fourier filtering, $\Delta S^{Mg-W}(Q)$ (red), $\Delta S^{Zn-W}(Q)$ (blue), and $\Delta S^{Mg-Zn}(Q)$ (green) b) Substracted background, using the same color code.

$\Delta S^{Zn-W}(Q)$ before the Fourier transform. This was found useful to limit ringing artifacts in the transformed r-space signal. We checked that this procedure did not affect peak positions (Fig. S2).

The neutron scattering experiments were duplicated on a different instrument, 7C2 at the Laboratoire Léon Brillouin (LLB) in Saclay) (FranceÃă for Mg^{2+} and the D20 (older version of the current D4) at the ILL in Grenoble (France) for Zn^{2+}. The obtained experimental data sets qualitatively exhibit the same features on the different instruments (Fig S3). The LLB experiment provided an even slightly shorter estimate for the Mg-O distance, around 2.0 Å. However, some unexpected behavior of the low-Q signal in this duplicated experiment makes us consider the ILL measurement as more reliable.

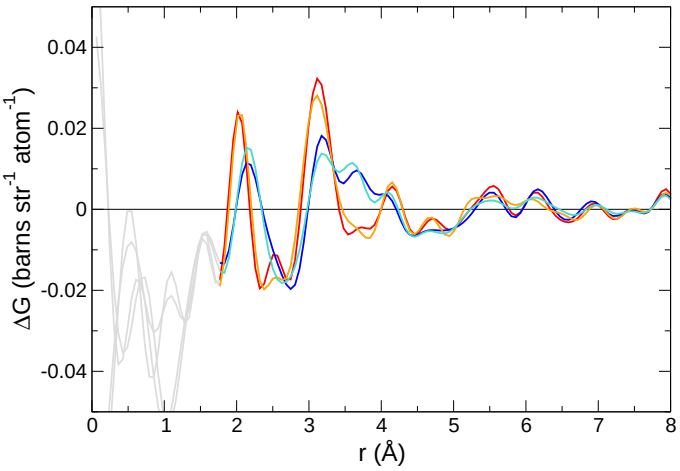

Figure S2: $\Delta G^{Mg-W}(r)$ and $\Delta G^{Zn-W}(r)$ without (red and dark blue) and with (orange and light blue) removal of two peaks in Q-space due to noisy detectors before the Fourier transform.

AIMD simulations

The influence of the dispersion correction (D3M(BJ)[1–3]) in the AIMD simulations was tested by repeating the Mg^{2+}–Cl^- and Zn^{2+}–Cl^- PMF calculations with a different dispersion correction, Grimme's original D2.[4] The obtained PMF are qualitatively consistent (Fig. S4), especially in terms of the free energy difference between CIP and SShIP, a key quantity in this work. However, the differences between the two calculations go beyond the estimated error bars, which suggests that these differences may not be only due to the limited sampling (less than 25 ps per window with D2) but also to the dispersion correction itself.

The accuracy of the employed level of DFT for Mg^{2+} was tested by optimizing the geometry $Mg(H_2O)_6^{2+}$ clusters (with a perfect Th symmetry) at different levels of theory in the gas phase, or using different solvent continuum descriptions (PCM[5] or CPCM[6]). All the calculations were performed with the Gaussian09 software.[7] The results are summarized in Table S1.

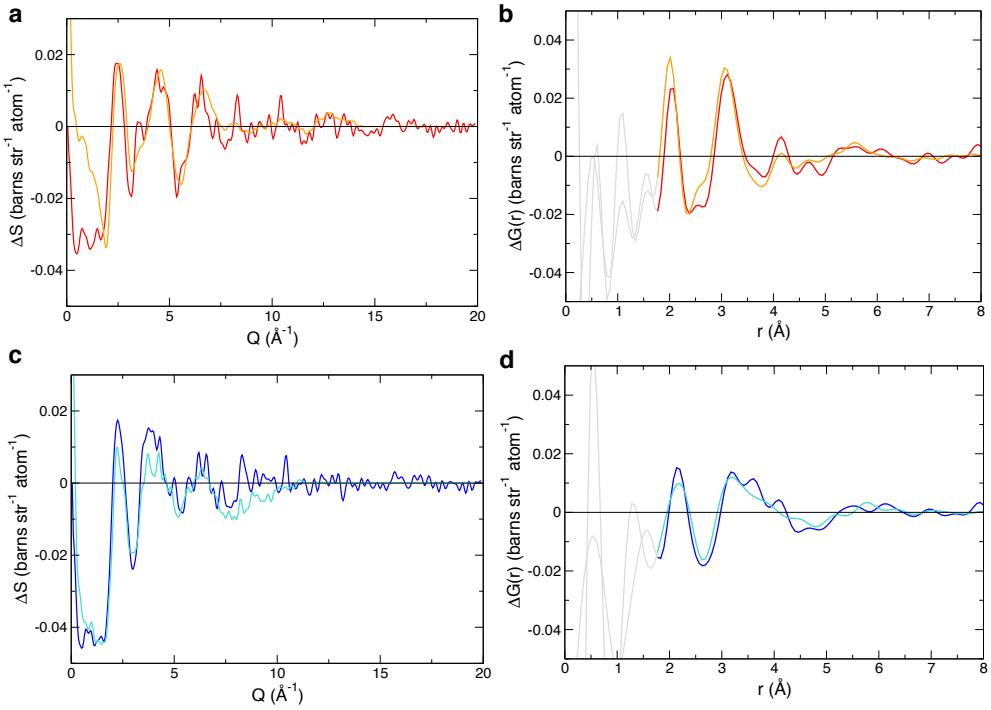

Figure S3: a) Comparison of the first order differences $\Delta S^{Mg-W}(Q)$ obtained from experiments performed on D4C in Grenoble (red) and 7C2 at the LLB in Saclay (orange) in Q-space. b) Same data in r-space. c) Comparison of the first order differences $\Delta S^{Zn-W}(Q)$ obtained from experiments performed on D4C (dark blue) and on the D20 at the ILL in Grenoble (light blue) in Q-space. d) Same data in r-space.

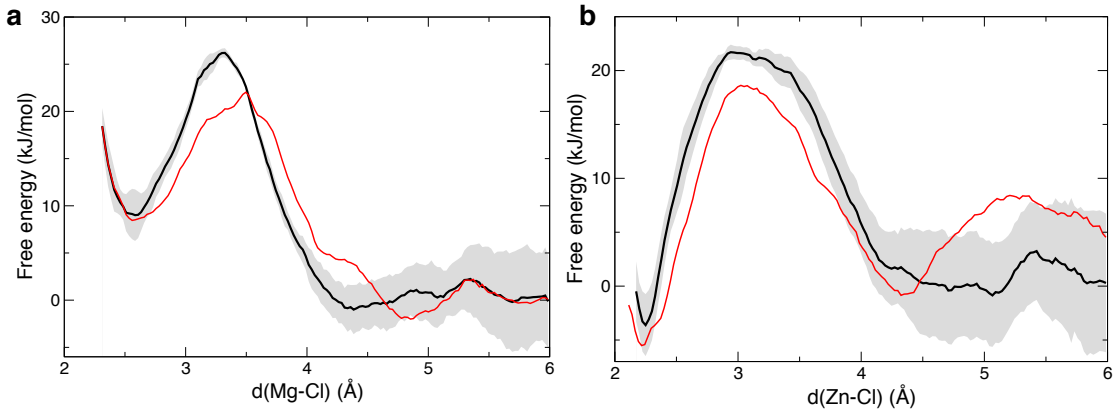

Figure S4: a) *Ab initio* free energy profile along the Mg-Cl distance using the D3M(BJ) (black) and D2 (red) dispersion correction b) *Ab initio* free energy profile along the Zn-Cl distance using the D3M(BJ) (black) and D2 (red) dispersion correction.

Table S1: Optimized Mg-O distance in $Mg(H_2O)_6^{2+}$ clusters with a perfect Th symmetry at different levels of theory

Level of theory	Basis set	d(Mg-O) (Å)		
		gas phase	PCM	CPCM
BLYP-D3	cc-pVDZ	2.097	2.051	2.069
	aug-cc-pVDZ	2.112	2.052	2.079
	cc-pVTZ	2.106	2.052	2.080
	aug-cc-pVTZ	2.108	2.052	2.084
B3LYP	cc-pVDZ	2.093	2.049	2.064
	aug-cc-pVDZ	2.105	2.051	2.075
	cc-pVTZ	2.098	2.050	2.069
	aug-cc-pVTZ	2.100	2.050	2.07
MP2(FULL)	cc-pVDZ	2.098	2.051	2.07
	aug-cc-pVDZ	2.084	2.045	2.055
	cc-pVTZ	2.072	2.040	2.046
	aug-cc-pVTZ	2.074	2.040	2.040
CCSD(FULL)	cc-pVDZ	2.098	2.051	2.07
	aug-cc-pVDZ	2.082	2.044	2.053
	cc-pVTZ	2.069	2.038	2.038

Comparison with the AMOEBA force field

Figure S5 shows how the Mg^{2+}–Cl^- and Zn^{2+}–Cl^- free energy profiles computed with the fully polarizable AMOEBA force field compare with those computed at the AIMD level and with our ECC description. For both cations, the AMOEBA and ECC description give comparable results. We note that, like ECC and full charges force fields, AMOEBA does not capture the stability of the $Zn^{2+}Cl^-$ contact ion pair.

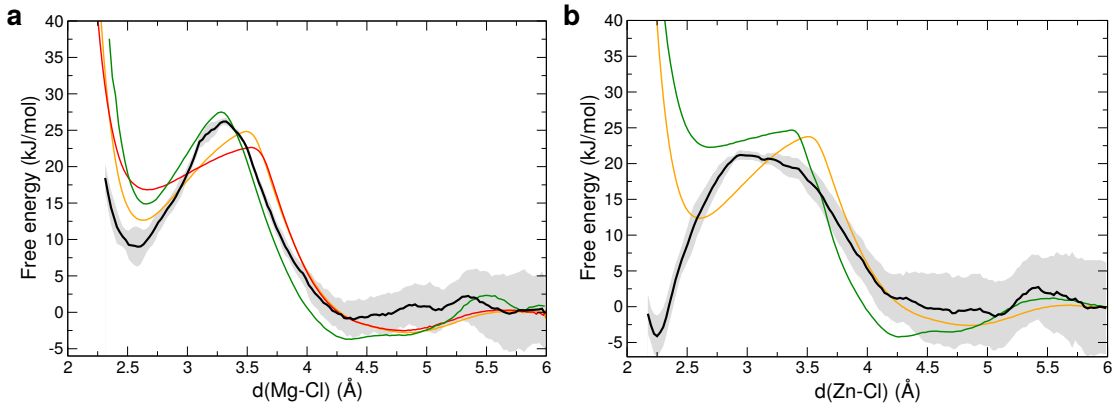

Figure S5: a) Free energy profile along the Mg^{2+}–Cl^{-} distance using *ab initio* MD (black), the "ECC big" (orange) and the "ECC small" (red) force fields, as well as the fully polarizable AMOEBA force field (green). b) Free energy profile along the Zn^{2+}–Cl^{-} distance using *ab initio* MD (black), the ECC (red) force field and the AMOEBA force field (green).

References

(1) Grimme, S.; Antony, J.; Ehrlich, S.; Krieg, H. A consistent and accurate ab initio parametrization of density functional dispersion correction (DFT-D) for the 94 elements H-Pu. *J. Chem. Phys.* **2010**, *132*, 154104.

(2) Smith, D. G. A.; Burns, L. A.; Patkowski, K.; Sherrill, C. D. Revised damping parameters for the D3 dispersion correction to density functional theory. *J. Phys. Chem. Lett.* **2016**, *7*, 2197–2203.

(3) Becke, A. D.; Johnson, E. R. A density-functional model of the dispersion interaction. *J. Chem. Phys.* **2005**, *123*, 154101.

(4) Grimme, S. Semiempirical GGA-type density functional constructed with a long-range dispersion correction. *J. Comput. Chem.* **2006**, *27*, 1787–1799.

(5) Tomasi, J.; Mennucci, B.; Cammi, R. Quantum mechanical continuum solvation models. *Chem. Rev.* **2005**, *105*, 2999–3093.

(6) Barone, V.; Cossi, M. Quantum calculation of molecular energies and energy gradients in solution by a conductor solvent model. *J. Phys. Chem. A* **1998**, *102*, 1995–2001.

(7) Frisch, M. J.; Trucks, G. W.; Schlegel, H. B.; Scuseria, G. E.; Robb, M. A.; Cheeseman, J. R.; Scalmani, G.; Barone, V.; Petersson, G. A.; Nakatsuji, H. et al. Gaussian09 - Revision D01. 2013.